A Theoretical Perspective of Vapor Interactions with Metal Surfaces

Christopher J Harris
Department of Chemistry
University of Maine

Abstract

There exists a variety of models to rationalize adsorption on transition metal surfaces. This paper will start by presenting an intuitive molecular orbital argument followed by a more quantitative density of states approach. Transition metals possess unique adsorption properties due to the enhanced d level interaction on the surface contributing to chemisorption. Predicting the strength of chemisorption effects falls in line with periodic features of the frontier d band. If the adsorption level becomes stronger than internal forces within the binding specie, the molecule breaks up. Therefore, density of states diagrams in conjunction with periodic trends offers the potential to tailor design catalysts.

Introduction

This paper will consist of two primary sections: the first part will describe a qualitative, visual interpretation of surface processes, while the second portion will apply these principles on a quantitative scale through a variety of computational approaches. Surface chemistry is at the foundations of all heterogeneous catalysis systems and could offer insight into film growth mechanisms.

Historically, films prepared by physical vapor deposition involve a vapor phase at one fixed composition to produce a uniform condensate material. However, creating a vapor in equilibrium with the solid state heavily constrains the growth conditions. Therefore, chemical vapor deposition, where reactants can be tailored to self limiting

steps, a wider growth window, and more precise composition gradients has emerged as a preferred method for film growth, through the control of surface chemistry.

Although this survey is by no means comprehensive, it covers a representative cross section of concepts encountered in surface chemistry. Emphasis will be placed on carbon monoxide and hydrogen interactions with metal surfaces, due to the cumulative data available, its characteristic behavior, and its potential in fuel cell catalysis.

Orbital View

Fortunately, surfaces exhibit the same types of phenomenon as large compounds or chemical clusters, and can be viewed as an extension of such systems. If one compares an unsaturated hydrocarbon to a metal surface, it would seem logical that the surface would want to arrange itself to optimize its structure based on its intrinsic coordination, consistent with a carbon chain. Clearly, if one introduced hydrogen to either system, the hydrocarbon chain or metal surface would rearrange itself to accommodate the higher level of saturation. In surfaces, this rearrangement to distinct crystal structures or to varying levels of saturation is called surface reconstruction[1].

Throughout the first part of this paper, Hückel theory will be used to explain surface phenomenon in much the same way that organic structures have come to light. Although electron cloud, self consistent fields are not preserved, the Hückel model yields reasonable energetic and structural trends on the surface, reflecting the inevitable coherence between chemistry, physics, and engineering[1].

Consider a slab of finite depth on a (111) surface of an fcc metal, as shown in figure 1. The stacking sequence in this hexagonal close packed system is ...ABCABC..., corresponding to the hollow space that each subsequent atomic layer chooses among the three hollow types available. In such a system, every third layer coincides with itself[1].

Looking down a Ni(100) surface in the plane of the page, figure 2 illustrates a typical c(2X2)CO adsorption pattern. Under these conditions, the carbon atom sits on every other nickel atom in both x and y directions, in accordance with a two by two

surface unit cell. Meanwhile, the oxygen atoms maintain a concentric orientation with the carbon atoms in the z direction, leading to an effective coverage of one half[1].

For simplicity, think about a pristine surface, containing atoms on the order of Avogadro's number. Each atom contributes valence orbitals consistent with the number of valence electrons present. As with other chemical phenomenon, the outermost valence electrons dictate the overall system properties. In one dimensional space, figures 3 and 4 depict hypothetical infinite hydrogen and carbon pi chains respectively. If you apply periodic boundary conditions, where one end connects to the other end, figure 5 shows the progression from bonds to bands, with the lowest energy level having the most bonding character, while the highest energy level exhibits the most antibonding behavior [1].

In fact, Bloch's theorem derives the band notion in a more explicit manner. For a one dimensional periodic array, as figure 6 shows, where n is a position index, a the lattice constant, k the momentum vector, and χ_n a basis set, such as H 1s or C 2p, the wavefunction ψ_k exhibits periodic behavior. If we evaluate the extremum at k = 0, π/a as figure 7 demonstrates, the most bonding and antibonding wavefunctions emerge. This unique interval, the Brillouin zone, $-\pi/a < k \leq \pi/a$, repeats itself outside that range[1].

Since the most bonding and antibonding wavefunctions would correspond to the lowest and highest energy levels, respectively, reciprocal lattice space leads us to the parallel between energy bands and an E-k diagram. In particular, figure 8 illustrates that a stack of energy levels, when multiplied by Avogadro's number, becomes an energy block, is equivalent to a quantum energy versus momentum plot. Reinforcing the parallel even further, each atom represents a unit cell in a pure one dimensional strand, so a one to one correspondence exists between the number of energy levels and allowed momentum or translation vectors[1].

Using reciprocal lattice space, let us return to CO adsorption on a Ni(100) surface, looking at individual E-k band diagrams of CO monolayer coverage, figure 9, and a Ni

(100) substrate, figure 10. These energy curves actually profile two dimensional momentum space by virtue of the k labels: $\Gamma(0,0)$, $X(\pi/a,0)$, $M(\pi/a,\pi/a)$, which represent the critical Brillouin zones in this crystal structure. When interpreting these band diagrams, it is helpful to visualize the equivalent atomic/ molecular orbital energy level diagram. For instance, the band diagram for CO encompasses all the familiar symbols for molecular orbitals, namely: 4σ, 1π, 5σ, $2\pi^*$, with the same energetic sequence[1].

One striking feature in figure 9 is the difference in overlap between the valence orbitals as the CO molecule spacing varies from half to full coverage. Clearly, orbital overlap increases as two molecules are brought together or as the energy between the two orbitals approach one another. The peaks within the band diagram for a particular orbital can be viewed as the most antibonding case while the valleys correspond to the most bonding situation. Therefore, the flatter bands would imply very little overlap relative to the steep, high band width, strong overlap orbitals. Weak intermolecular overlap produces narrow bands, localizing the electrons to diminish conductivity. Conversely, strong intermolecular overlap creates wide bands, where electrons delocalize to enhance conductivity[1].

When viewing figure 10, one is overwhelmed by the profusion of energy bands. For CO, it only reaches a monolayer thickness, so it only has one molecule per unit cell or one set of valence orbitals, while the 4-layer nickel slab contains 4 atoms per unit cell with each atom possessing a full set of 3d, 4s and 4p valence orbitals. From the behavior of the Ni energy bands, it would appear that the relatively flat 3d valence orbitals near the bottom of the band diagram, do not conduct electrons as well as more diffuse 4s and 4p valence orbitals near the upper end of the energy spectrum. Another prominent feature that differentiates the 4-layer nickel slab from the monolayer CO relates to the intertwining between different bands, meaning electrons can take on any energy up to continuum, symbolic of a conductor[1].

Rather than make a band by band analysis of the system, it is usually more effective to consider a composite density of states (DOS), which is defined by:

DOS(E) = number of levels between E and E+dE .

Figure 11 shows the transformation from a band diagram to its density of states for a basic one dimensional hydrogen chain. Since the energy levels are evenly distributed among k values in a band diagram, the flatter regions accumulate more states than do steeper areas. Therefore, from a mathematical point of view, the density of states is inversely proportional to the slope of the band diagram[1].

If you integrate the density of states up to the Fermi level, then you know the number of occupied molecular orbitals. Applying Pauli's exclusion principle, the number of occupied molecular orbitals times two represents the total number of valence electrons. Thus, the density of states depicts the electron energy distribution, the Mulliken population, at a glance. As an example, figure 12 demonstrates the relationship between a band diagram and density of states for the half coverage CO monolayer, confirming sharp electron peaks, consistent with localized electrons. One consequence of the transformation between E-k reciprocal lattice space to density of states brings the system back to real space, as started with in the unit cell[1].

Up until now, only the separate band diagrams for monolayer CO and Ni(100) have been displayed. From a density of states perspective, figure 13 conveys how the two systems interact with one another. On both extremes, the pure noninteracting systems are presented, but in the center, where the c(2X2)CO-Ni(100) attains realization, a direct superposition of density of states does not occur. Although the DOS for the nickel slab remain fairly intact, the 5σ from the monolayer CO drops in energy, while the $2\pi^*$ orbital becomes somewhat obscured[1].

If we zero in on the contributions that the 5σ and the $2\pi^*$ orbitals make within the c(2X2)CO-Ni(100) framework, as figure 14 depicts, the 5σ has an electron occupation of 1.62, while the $2\pi^*$ has an occupation of 0.74 . These values are obtained by applying the integration process up to the Fermi level and multiplying by 2, assuming the the Fermi level should be close to the center of the noninteracting band, which is

superimposed in figure 14, along with the integration level[1].

So, how does this tie into our simple model of a CO ligand in a metalorganic system? As outlined in figure 15, typically, the 5σ orbital on CO donates electrons to the metal d orbitals, which in turn, back donate these electrons to the CO 2π* orbitals. On the surface, when you match up the symmetry related metal orbitals to the CO molecule, as figure 16 does, a similar mechanism becomes evident. More specifically, the Ni d_{z^2} will have a sigma bond interaction with the CO 5σ, while the Ni $d_{xz,yz}$ should have a pi bond interaction with the CO 2π*. Again, the two end diagrams represent the pure noninteracting cases, while the central images show the interaction outcome for the particular valence orbitals involved. Clearly, the Ni d_{z^2} orbitals take on a resonance where the CO 5σ should reside, indicating some sort of electron exchange. However, a more dramatic response takes place between Ni $d_{xz,yz}$ and CO 2π*, where both sides reveal resonances originating from the other species[1].

Perhaps some bonding theory might explain why 2π* has a more pronounced interaction than 5σ. In earlier discussion, it was pointed out that overlap increases as two molecules come together or as the orbital energies approach one another. More formally, perturbation theory states:

$$\Delta E = \frac{\left| H_{ij} \right|^2}{E_i^0 - E_j^0} \quad .$$

where: ΔE = *interaction energy*

H_{ij} = *Hamiltonian integral between i and j*

E_i^0, E_j^0 = *orbital energy for species i and j*

Symmetry plays a role as well, particularly in the normalization of the overall wavefunction:

$$\psi_\pm = \frac{1}{\sqrt{2(1\pm S_{12})}}(\phi_1 \pm \phi_2) \ .$$

where: ψ = *overall wavefunction*

              S_{12} = *overlap integral between 1 and 2*

              ϕ_1, ϕ_2 = *basis set for species 1 and 2*

From an energetic argument, the difference between CO 5σ and Ni d_{z^2} orbitals is about the same as the gap between CO $2\pi^*$ and Ni $d_{xz,yz}$. Perhaps symmetry imposes a broader influence since the latter pair involves two nickel d orbitals[1].

Although normalization of the overall wavefunction contains relevant information concerning symmetry, the cross term involving the overlap integral may provide a more visual interpretation of bond preferences. Take for instance a two component orbital:

$$\psi = c_1 \phi_1 + c_2 \phi_2 \ ,$$

upon normalization:

$$\int |\psi|^2 \, d\tau = 1 = \int |c_1 \phi_1 + c_2 \phi_2|^2 \, d\tau = c_1^2 + c_2^2 + 2c_1 c_2 S_{12} \ ,$$

where: ψ = *overall wavefunction*

              τ = *volume element*

              c_1, c_2 = *distribution coefficients*

              ϕ_1, ϕ_2 = *basis set for species 1 and 2*

              S_{12} = *overlap integral between 1 and 2*

yields the cross term, $2c_1 c_2 S_{12}$, which scales according to Pauli's bond order

concept. When applied to the solid state realm, the crystal orbital overlap population, COOP for short, looks something like figure 17 in our fledgling hydrogen chain, where a particular bond must be specified. One defining element in a COOP curve attributes negative regions to antibonding and positive regions to bonding. Thus, the crystal orbital overlap population depends on the number of states at a particular energy level, molecular orbital coefficients, and the overlap integral. If you integrate the COOP curve up to the Fermi level, the total overlap population results, a quantity analogous to bond order in crystals[1].

Figure 18, a crystal orbital overlap population for c(2X2)CO-Ni(100), reinforces the notion of a CO ligand in a metalorganic system, as the 5σ bonds with a low lying Ni d orbital, while the $2\pi^*$ bonds with higher level Ni d orbitals, reminiscent of a sigma donation, followed by a pi back donation. Even the polarity of the orbitals can be resolved from a COOP curve, as the sigma bond involves two bonding orbitals, while the pi bond contains CO antibonding orbitals in combination with Ni d bonding orbitals. In a face centered cubic lattice, the Ni atom should have close to a tetrahedral environment, so this picture is consistent with ligand field theory, where d_{z^2} orbitals lie below higher energy $d_{xz,yz}$ [1].

Perturbation theory has the leverage to reveal macroscopic behavior through interactions between highest occupied molecular orbitals (HOMO), and lowest unoccupied molecular orbitals (LUMO), which represent the frontier orbitals within the system. Whenever an orbital interaction transpires, both a bonding and an antibonding level results, as figure 19 attests. Keep in mind the antibonding orbital ascends higher in energy than the bonding orbital drops, so electron populations determine the viability of a specific interaction[1].

In a molecular system, figure 20 shows the four conceivable frontier orbital exchanges. Interactions 1 and 2 signify a two electron exchange, with advantageous energy consequences leading to bonding. If the electron spacial resolution and energy balance, a covalent bond results, whereas unequal partners lead to electron transfer, a

dative bond transaction. Interaction 3 represents a four electron exchange, which inevitably becomes repulsive, as bonding and antibonding levels fill according to figure 21, creating an energetically unfavorable situation, commonly seen in steric hindrance or lone pair repulsion scenarios. Finally, interaction 4, a zero electron exchange between two unfilled levels, has no energetic outcome with respect to molecules[1].

Up until now, very little has been said concerning the Fermi level, which plays a pivotal role in surface interactions. By definition, the Fermi level represents: the chemical potential of electrons at absolute zero temperature, the highest level of filled electron states for 0 K, or the energy surface in a vast sea of electrons. If the Fermi energy intersects a band anywhere across a band diagram, that material has conductive behavior, as unoccupied states exist immediately above the ground state to accommodate electron/ hole transport[1].

When a surface replaces an atom, orbital interactions occur between an adsorbate atom with discreet energy levels and the electron band associated with the surface, in parallel with figure 22b. Due to the presence of the electron band, interactions 3 and 4 may become attractive, while a new interaction 5 emerges about the Fermi level. Again, interactions 1 and 2 remain bonding, whether the electron source originates from an atom or a band. For interaction 3, if the antibonding perturbation energy exceeds the Fermi energy, then electrons flow into the band at the Fermi level, consistent with figure 23b, creating a bonding exchange. When the bonding perturbation energy drops below the Fermi energy as interaction 4 develops, then electrons flow out of the band into the bonding level, in accordance with figure 24b, producing an attractive outcome. The flux of electrons flowing into and out of energy bands at the Fermi level, and subsequent exchange between internal or uncoordinated surface atoms to balance the electron distribution, may derive bonding and antibonding forces in metallic solids, attributed to interaction 5 [1].

Through the surface interactions developed here, fundamental events, such as: chemisorption barriers, bonding compromises, surface site preferences, and Fermi level

influences take shape[1]. Instead of presenting the issues systematically, perhaps a few practical examples will address these concerns from a more realistic perspective. Therefore, the remainder of the paper will highlight computational resources and their application to surface catalysis.

Numerical Strategies

Although the Hückel model portrays a semiempirical approach to electronic structure calculations, ab initio techniques provide greater accuracy. By design, the ab initio method requires just atomic numbers as input, calculating the results through quantum mechanical, first principles, rather than experimental parameters. One such variation on this theme involves density functional theory, where hypothetical noninteracting molecular orbitals replace typical interactive wavefunction based systems. By making the molecular orbitals noninteracting, the Schrödinger relation for each electron becomes independent, simplifying the mathematics. Then one solves the Schrödinger equations for the electron density, proportional to the wavefunction squared [2,3,4].

The density functional method relies on finding a suitable functional for the system involved, to produce a ground state energy corresponding to the electron density. If excited states need consideration, a time dependent, density functional approach broadens the field beyond the ground state. In the process of creating a functional, jellium experiments must be referenced to determine the electron density-ground state energy relationship. Thus, some would argue that density functional theory is not a pure ab initio procedure. However, the economies of scale allow it to: handle larger systems, simplify the mathematics, and take into account electron correlation, while maintaining the same level of accuracy as traditional Hartree-Fock techniques[2,3,4].

For adsorbate-surface ensembles, two strategies exist to simulate the interaction, either the cluster model, where up to 50 atoms collectively represent the system, or periodic slab model, containing 3 to 5 layers of atoms, separated by a substantial vacuum

region to isolate the surface regions from one another, under periodic boundary conditions. Clearly, 50 atoms remains well short of even nanoparticle systems, which range up to 1000 molecules, but the advantage to this approach lies in the direct calculation of orbitals, from which bond strengths and forces become apparent. Meanwhile, the layer algorithm involves plane waves, which no longer have local significance, so orbitals become somewhat difficult to resolve. In practice, slab calculations give more reliable long range molecule-surface energetics, while the cluster method yields localized structure information and vibration frequencies, making them complementary techniques[2,3].

In dealing with transition metal surfaces, the free electron model provides a realistic reference frame towards interpreting density functional results. Typically, the s band has a broad weak overlap reflected in the density of states, while the d band exhibits a strong distinct overlap due to the combination of sigma and pi orbital interactions within the lattice, characterized by figure 25. When the two bands on the transition metal surface encounter an adsorbate, the s band broadens the adsorbate density of states within a single bonding mode, as in figure 26a, while the d band creates a sharp bonding and antibonding level within the adsorbate, consistent with perturbation theory, figure 26b [3,5].

The continuity between the single bonding mode, weak chemisorption state, and the dual level, strong chemisorption state is depicted in figure 27. Below the density of states sequence, a corresponding oxygen(2p)-palladium(3d) interaction curve illustrates how the d band center factors into the model. In a weak chemisorption situation, the adsorbate density of states is predominantly bonding over a broad energy spectrum, as it responds to the delocalized d band. To preserve the number of electrons, the area under the density of states curves for both the adsorbate and the metal below the Fermi level remains fixed throughout the chemisorption phases. Keeping the electron fill level constant, the d band center moves up toward the Fermi level as the metal d band overlap becomes more pronounced, inducing an antibonding peak to emerge within the

adsorbate. When these antibonding states protrude beyond the Fermi level, the bonding interaction ultimately strengthens. Due to weak, relatively uniform s band interactions, d band overlap dominates the bonding behavior in transition metals. Parameters such as d band center, electron fill level, and d band width serve as guidelines toward bond viability, influenced by shifting bonding states below the Fermi level or elevating antibonding states above the Fermi level[3,5].

As a first pass at evaluating periodic trends in reactivity, figure 28 explores the oxygen chemisorption energies for late transition metal surfaces in close packed structures. By definition, chemisorption energy represents the final energy state minus the two initial energy configurations:

$$E_{chem} = E(O/surface) - E(O\,atom) - E(surface)\ .$$

Since the bond energy per oxygen atom in O_2 is about -2.95 eV, as represented by an arrow on the ruthenium energy curve, it would appear that oxygen stays in its molecular form on the gold surface. For all the other transition metals considered, the bond strength between the surface and atomic oxygen exceeds the O_2 bond energy, so dissociation ensues. Clearly, progressing right along a row, or traversing down a column, the chemisorption energy declines within the transition metals[3].

The corresponding density of state diagrams for oxygen on transition metal surfaces, figure 29, reveals the underlying periodic contribution to chemisorption energy. Moving left from Cu/Ag/Au, the metal d band approaches, then surpasses the Fermi level, driven by the electron population. Consequently, the oxygen p orbital states transfer a larger share of electrons to the metal d band, sweeping the antibonding states above the Fermi level, to strengthen the bonding interaction. The depletion in surface d band occupation increases the capacity for adsorbate electron flow, enhancing the bonding potential[2,3].

Figure 30 demonstrates the progression of orbital interactions leading to chemisorption, bounded by an oxygen molecule on the left and a platinum surface to the

right. When the adsorbate encounters the diffuse sp metal band, a weak bonding interaction results. As the metal d band imposes its field, bonding and antibonding peaks coalesce within the oxygen $2p_x$ spectrum, reminiscent of the free electron model. Collectively, these orbital interactions realize the density of state diagrams presented in figure 29 [3].

Under scrutiny, density functional theory shows reasonable agreement with more basic models and experiment. For example, in the transition metal row: Zr through Ag, a linearly declining relationship exists for the oxygen chemisorption energy, consistent with figure 31. As the metal d band fills, the adsorbate antibonding peaks no longer have a reservoir to empty their states. In parallel with the transition metal position along a row, the d band: center, width, or fill level, produce a comparable linear relationship, applying free electron principles[2,3].

To rationalize column periodicity among transition metals, the overlap integral plays a key role in determining how the oxygen chemisorption energy behaves, figure 32. Because Cu/Ag/Au possess a completely filled d band, adsorbates have no place to dump their populated antibonding states, minimizing the bonding effects. Adhering to Pauli's exclusion rule, the metal d bands orthogonalize with the oxygen $2p_x$ orbitals upon interaction, to avoid same state occupation, which enhances repulsion. The overlap integral obtained from perturbation theory suggests that repulsion should increase with electron shell layers, so gold experiences the most dramatic electron repulsion, appearing as the noblest metal to oxygen. However, the overlap integral reinforces bonding interactions as well as electron repulsion, so for less electronegative adsorbates, bonding could overwhelm repulsion, making Ag or Cu the most passive surface[2,3].

For molecular adsorbates, such as carbon monoxide, the density of states analysis remains about the same, except that valence electrons populate molecular orbitals. At a first glance, there exists a remarkable similarity between figure 30, an atomic adsorbate and its molecular counterpart, figure 33. Since aluminum does not possess d band electrons, its only contribution lies in the sp coupling, which produces an energy drop,

characteristic of a weak chemisorption interaction. In response to the energy shift, the 5σ CO valence states converge with the 4σ molecular orbitals, enhancing the structure on the 5σ energy spectrum. Progressing from aluminum to platinum, the carbon monoxide experiences a combination of sp and d band influence, so bonding/ antibonding peaks develop on the energy landscape of both the 5σ and $2\pi^*$ CO orbitals. Because the 5σ CO bonding/ antibonding states appear primarily below the Fermi level, they cancel one another out, yielding no net attraction. In contrast, only the bonding levels in $2\pi^*$ CO orbitals populate, creating an overall attractive force[2,3].

Moving to the left within a row of the periodic chart for a transition metal, the same trends apply to molecular adsorbates as observed in atomic chemisorption. When the metal d band progressively depopulates, the attractive force strengthens between the surface and the adsorbate until the internal forces can no longer hold the molecule together. Thereafter, the adsorbed species breaks into its atomic components on the surface, as illustrated in figure 34 for both CO and NO. Clearly, the threshold between molecular and atomic chemisorption depends on internal forces within the molecule, so this transitional point will vary for each given adsorbate[3].

Whether dealing with atomic chemisorption, molecular chemisorption, or subsequent surface reactions, the density of states template provides the necessary framework to determine relative bond strengths or energy barriers. To analyze reactivity, the energy profile at the transition state geometry represents the minimum energy, reaction pathway. Consider figure 35, which shows the energy landscape for hydrogen decomposition among the four transition metal catalysts: nickel, platinum, copper, and gold. Hydrogen readily decomposes on Ni and Pt surfaces, but experiences progressively higher energy barriers between Cu and Au. As the metal d band center approaches the Fermi level, the activation energy subsides, because the hydrogen molecular orbitals interact more favorably with the surface d orbitals, disrupting the molecular integrity. Again, row and column periodic trends associated with chemisorption apply equally well to reaction barriers. Moving to the right along a row populates the metal d band, while

traversing down a column enhances electron repulsion, so both activities promote the transition state energy[3].

With heterogeneous catalysis, the six steps that need close attention include: transport to the substrate, adsorption, diffusion on the surface, surface reaction, desorption, then transport away from the substrate. The process which has the slowest rate or highest activation energy represents the rate limiting step. Under optimum conditions, the rate limiting step typically narrows down to the formation of a key reaction intermediate or its associated heat of adsorption[2,3,6].

To evaluate the catalytic activity of a particular substrate, a plot of the overall reaction rate versus the adsorption enthalpy of the critical component leads to a volcano plot, depicted in figure 36. The goal in choosing the ideal substrate follows Sabatier's principle: a surface with a low adsorption heat will bind so strongly that the product never evolves, while a substrate with a high adsorption enthalpy contains too few reaction intermediates to allow kinetics to flourish. Somewhere in the middle represents the optimal catalytic activity and selectivity. Sites closest to the optimum energy tend to dominate the reaction kinetics, making it relatively simple to model the system based on the preferential behavior. If the reaction parameters stray from ideal conditions, the reaction order changes continuously, having a positive reaction order below the optimal level and negative reaction order above the optimum activity, consistent with the parabolic shape. Various techniques exist to modify adsorption enthalpy through multicomponent surfaces, dopants, stress/ strain, and crystal morphology[2,3,6].

Conclusion

This paper has sought to make a connection between molecular orbital diagrams and density of state pictures. Regardless of approach, frontier orbitals or Fermi level states dictate the ultimate behavior of a chemical system. Using electron diagramming tools, adsorption and surface reaction trends become discernible to allow the design of an ideal catalyst.
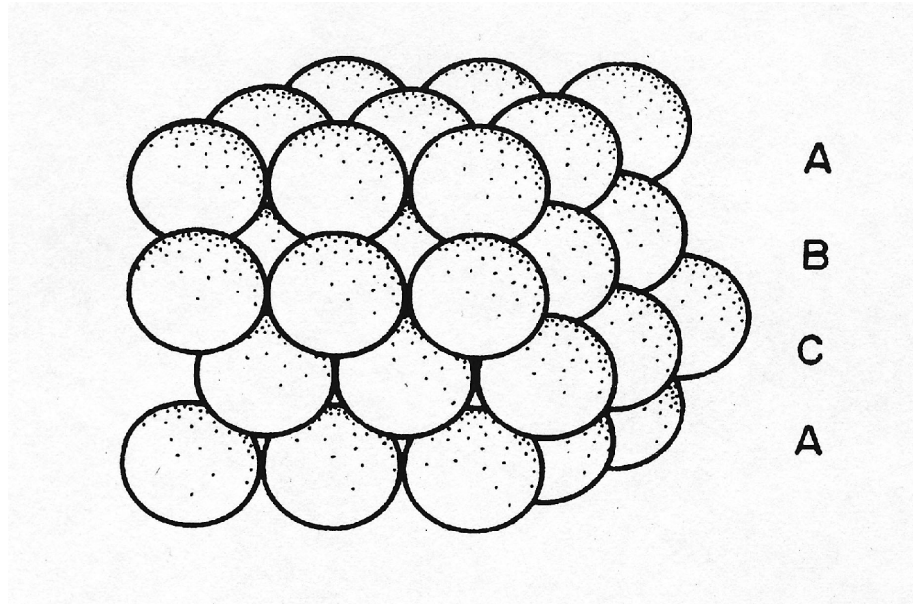
Figure 1:   Stacking sequence for a hexagonal close packed fcc metal.
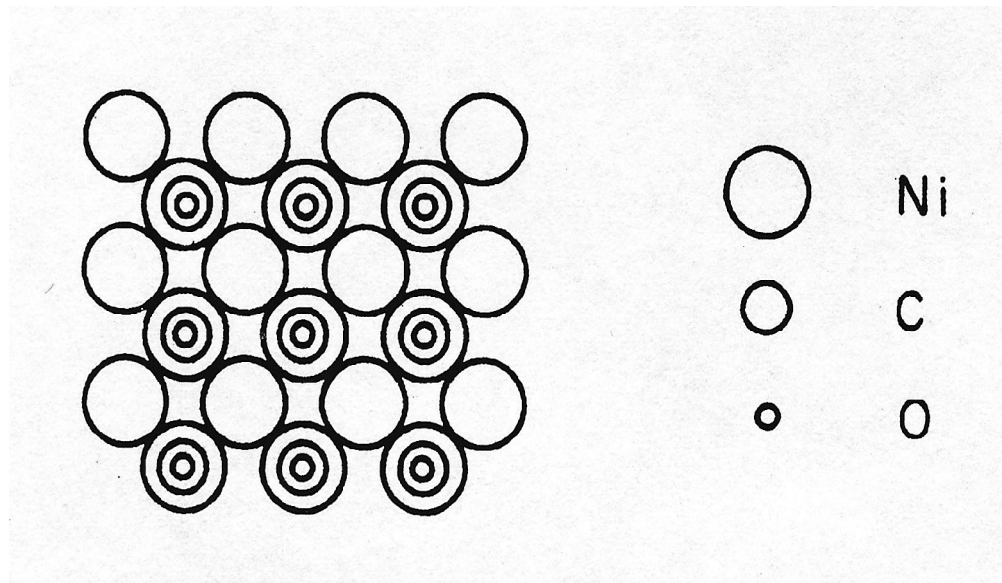
Figure 2:   Top view of carbon monoxide adsorbed on a nickel surface.
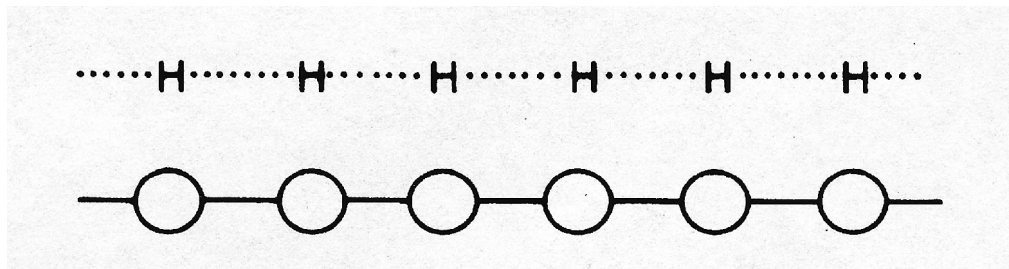
Figure 3: Idealized 1s basis set, hydrogen chain.
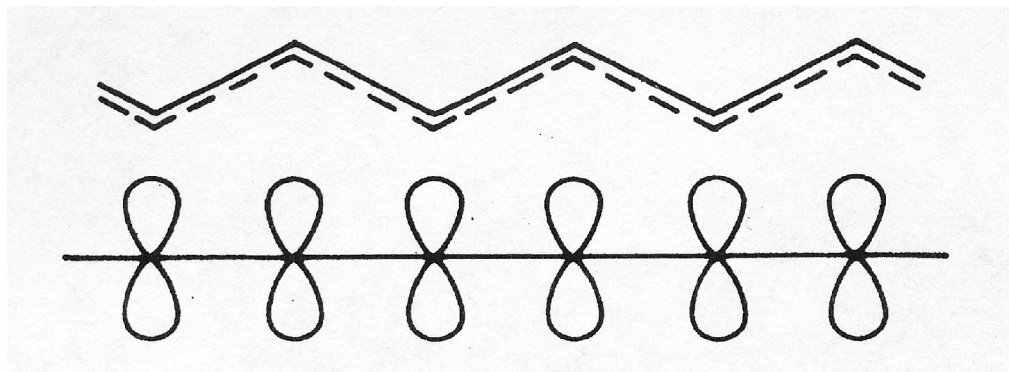
Figure 4: Infinite carbon pi chain.
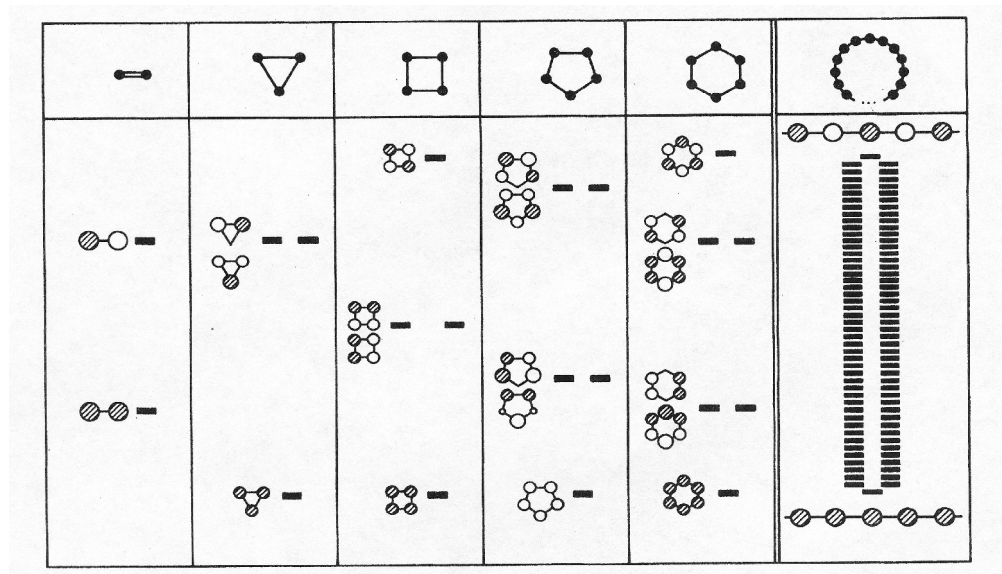
Figure 5:   Transition from bonds to bands.

$$\psi_k = \sum_n e^{ikna} \chi_n$$
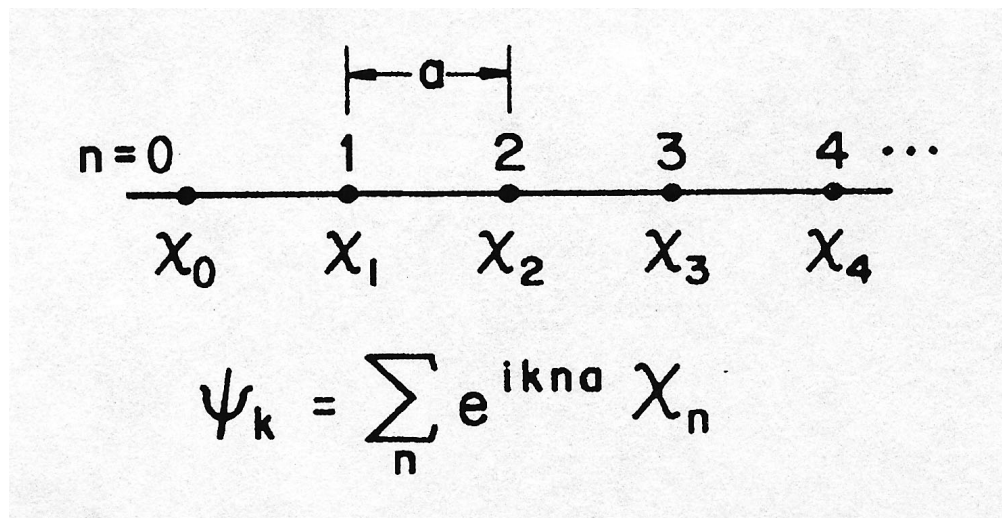
Figure 6:   Bloch's theorem for a one dimensional array.

$$k = 0 \qquad \psi_0 = \sum_n e^0 \, X_n = \sum_n X_n$$

$$= X_0 + X_1 + X_2 + X_3 + \cdots$$

$$k = \frac{\pi}{a} \qquad \psi_{\frac{\pi}{a}} = \sum_n e^{\pi i n} \, X_n = \sum_n (-1)^n X_n$$

$$= X_0 - X_1 + X_2 - X_3 + \cdots$$
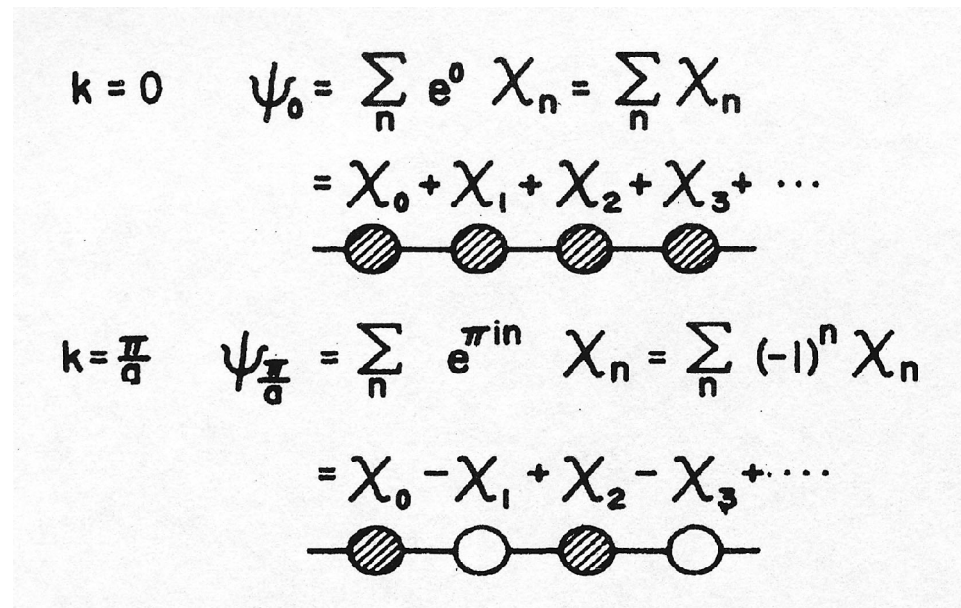
Figure 7:   Extreme limits in Bloch's function, known as the Brillouin zone.
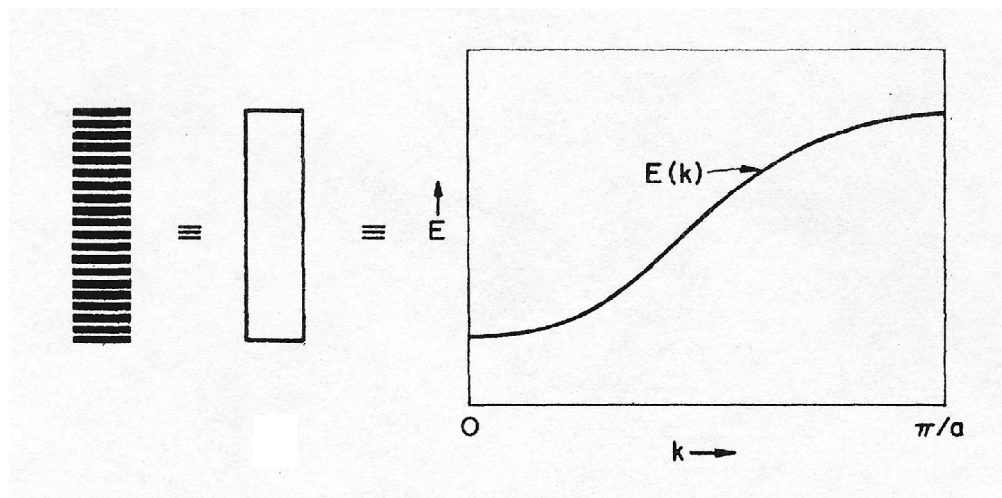
Figure 8:   The equivalence between energy levels, a ban
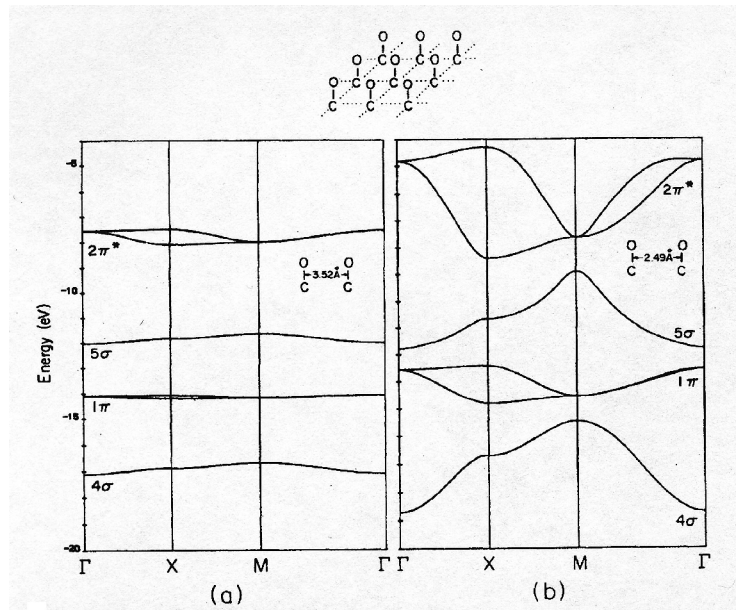
Figure 9:   Band diagram for CO on a Ni surface at two distinct molecular distances corresponding to (a) half and (b) full coverage
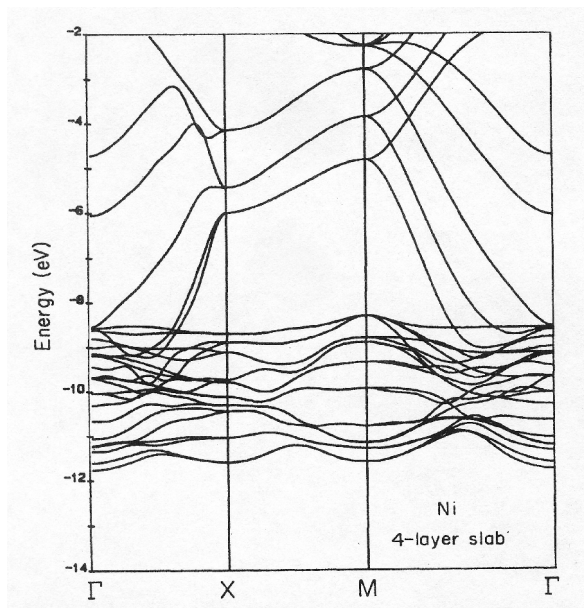
Figure 10: Underlying nickel substrate valence band.
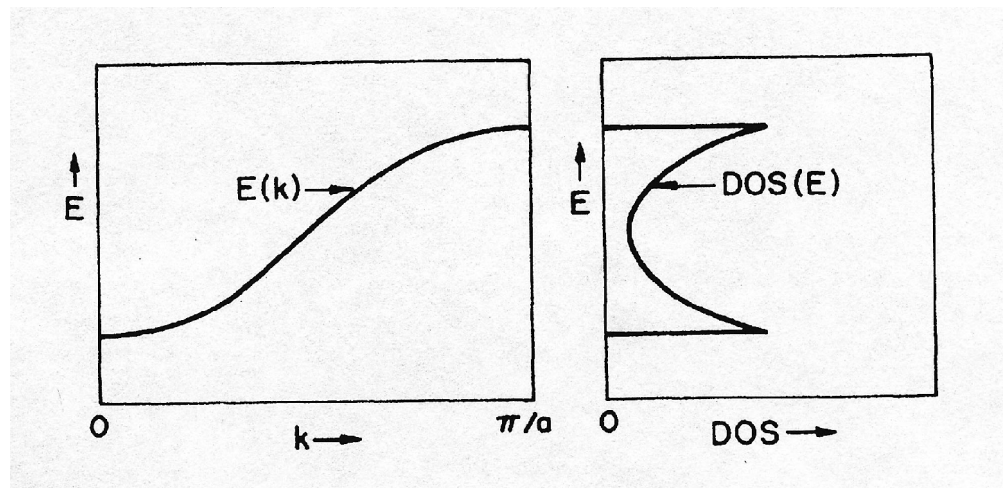
Figure 11: Parallel between E-k space and density of states for a cyclic
hydrogen chain.
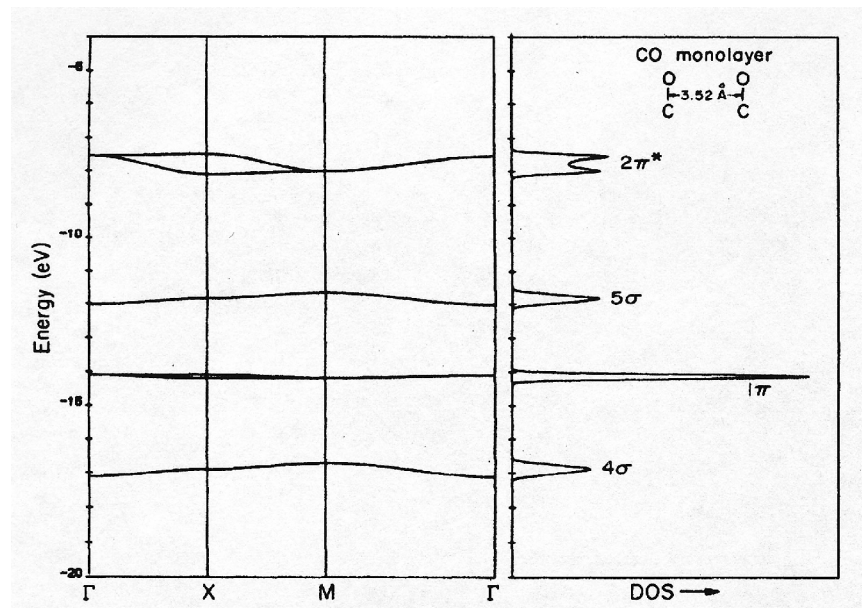
Figure 12: Band pattern and its comparable density of states image for half
coverage CO bound to a nickel surface.
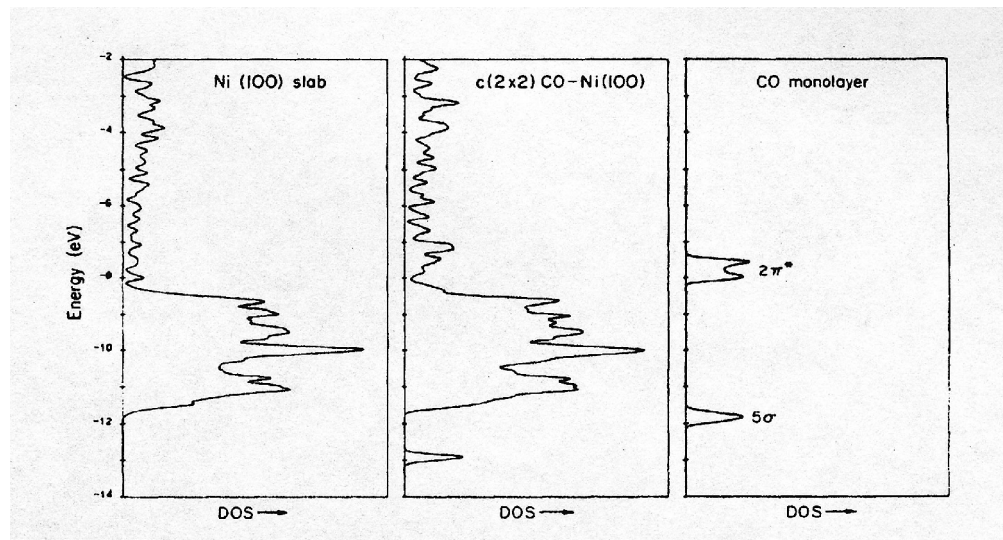
Figure 13: From left to right, density of states for the nickel substrate, CO adsorbed on Ni, and CO alone.
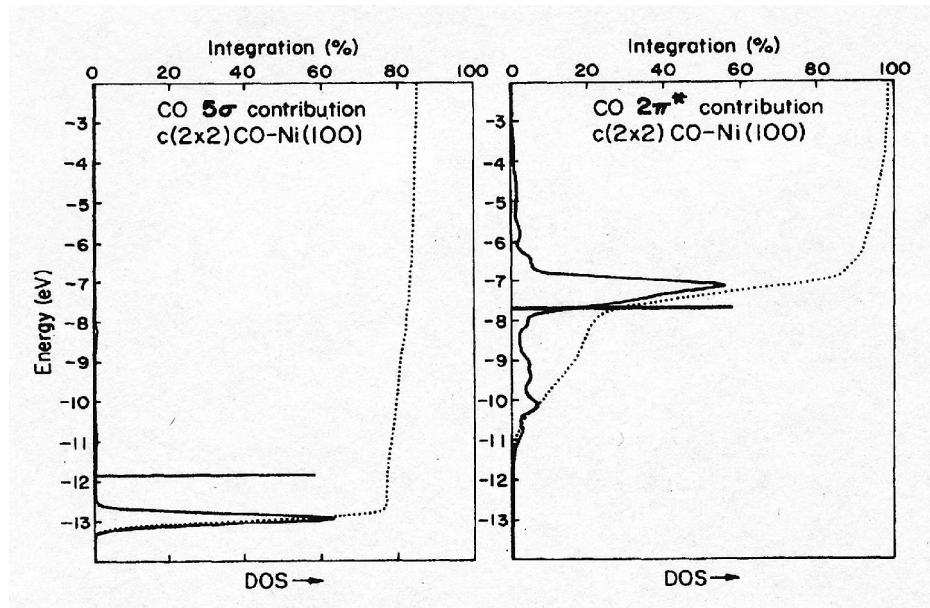
Figure 14: Participation level of the carbon monoxide molecular orbitals.
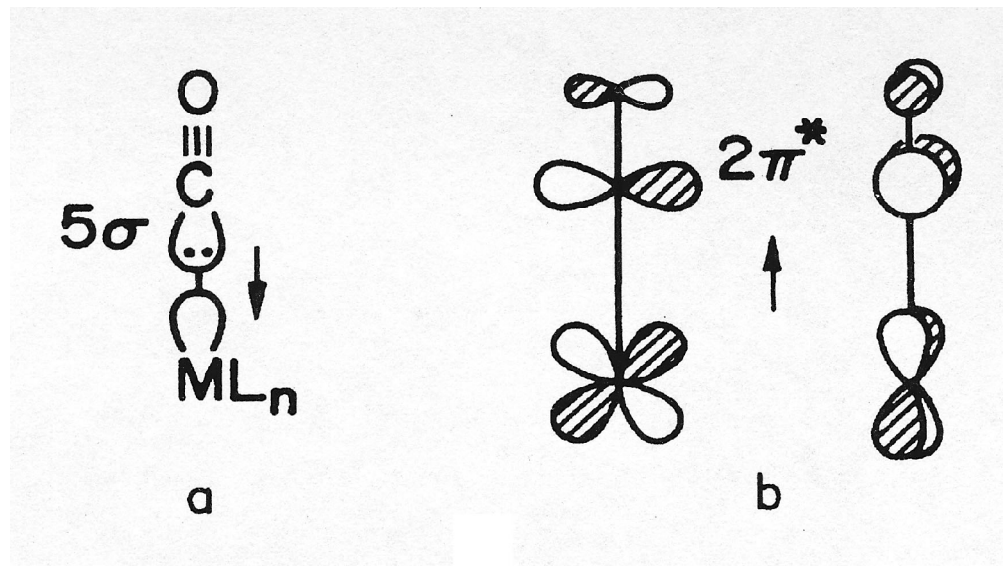
Figure 15: Organometallic view of valence electron flow for a CO ligand.
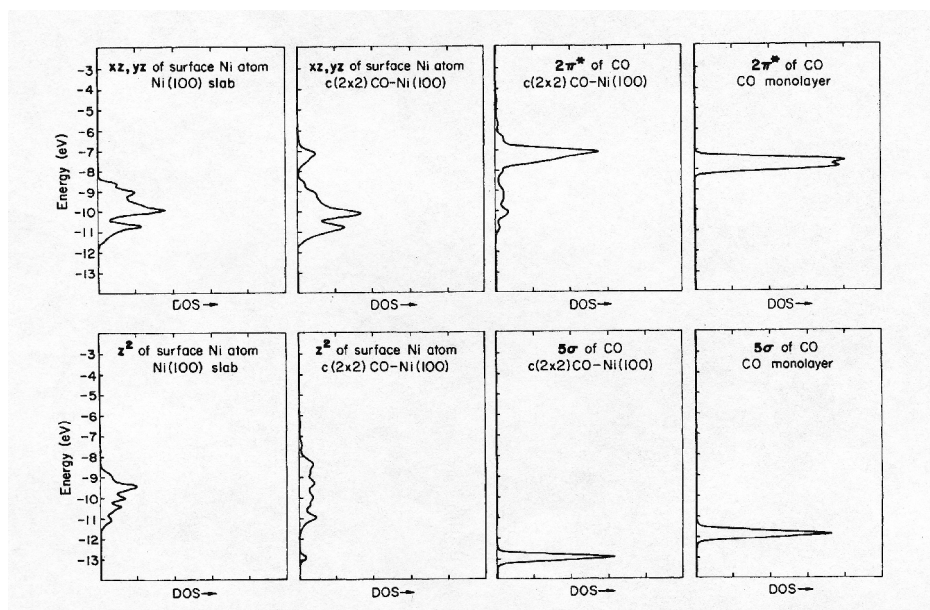
Figure 16: Symmetry related transformations between the nickel and carbon
monoxide valence orbitals upon adsorption.
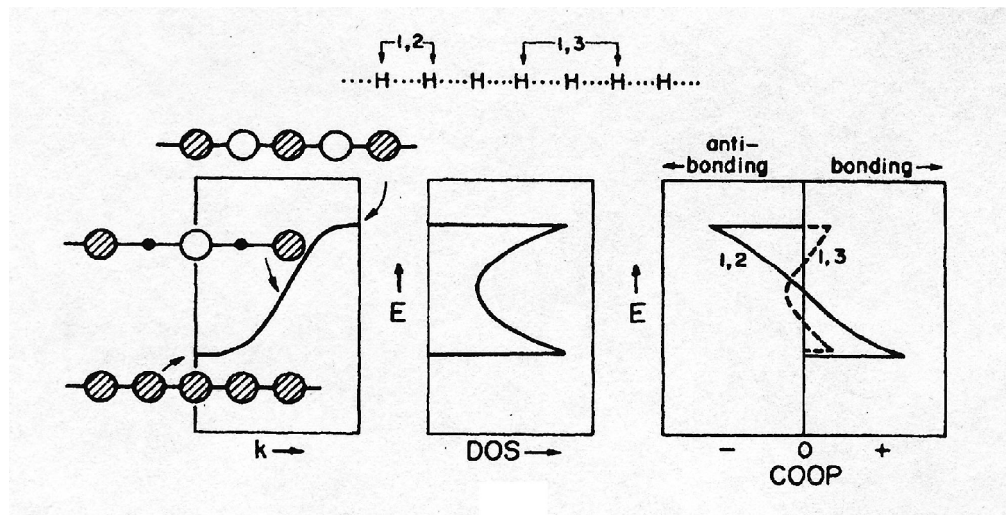
Figure 17: Interchangability between k-space, density of states, and crystal orbital overlap population in a hydrogen chain.
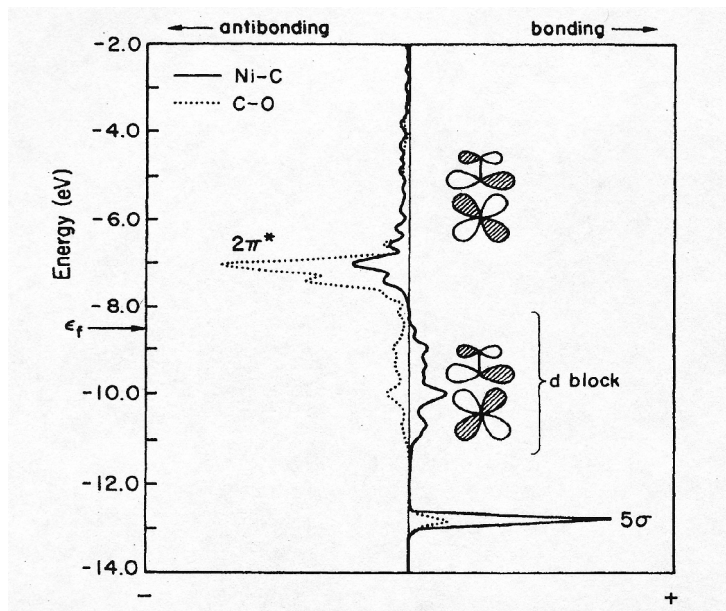
Figure 18: COOP curves for the Ni-C and C-O bonds illustrating frontier orbital interactions.
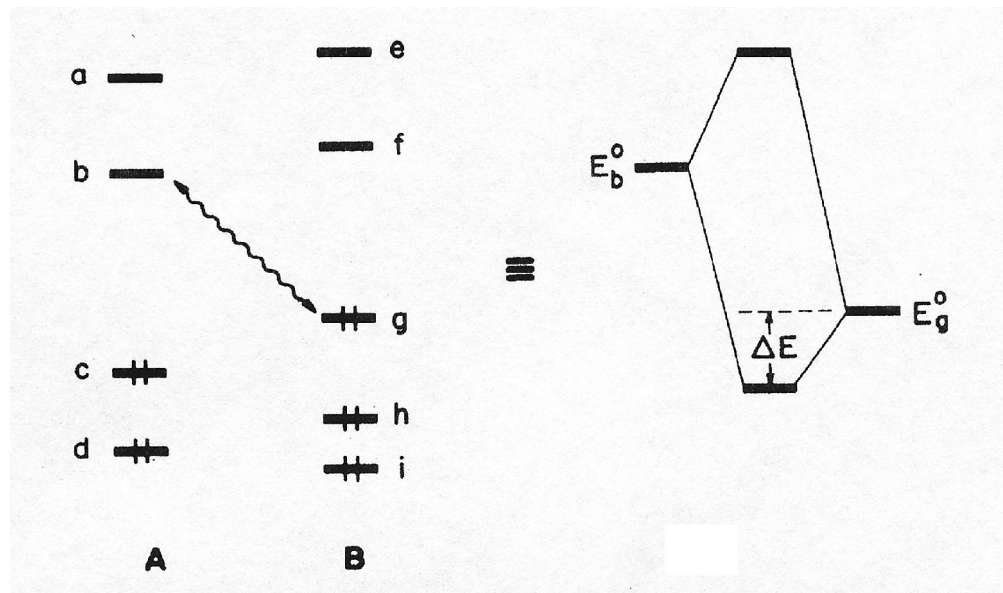
Figure 19: An energetically favorable electron shell exchange between two atoms within a molecule.
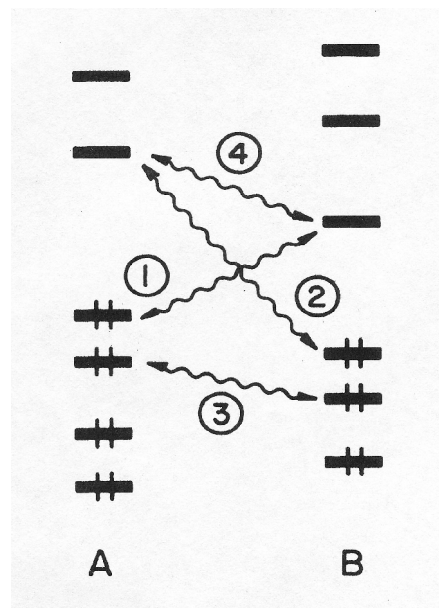
Figure 20: All possible frontier orbital combinations in a molecular system.
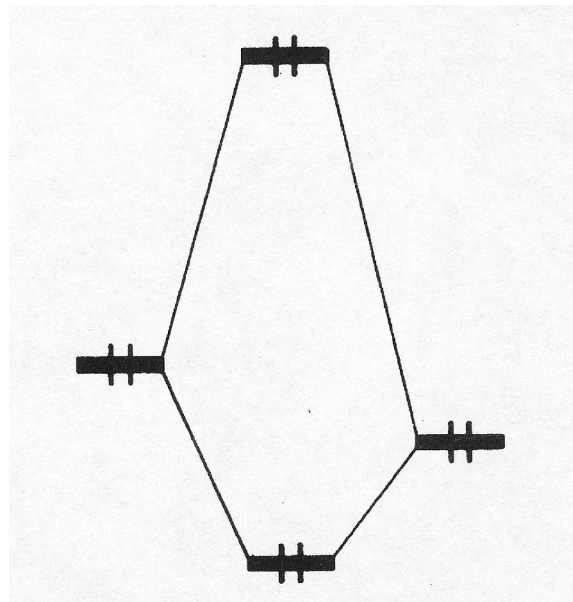
Figure 21: Perturbation consequences between two atoms with filled orbitals in a molecular framework.
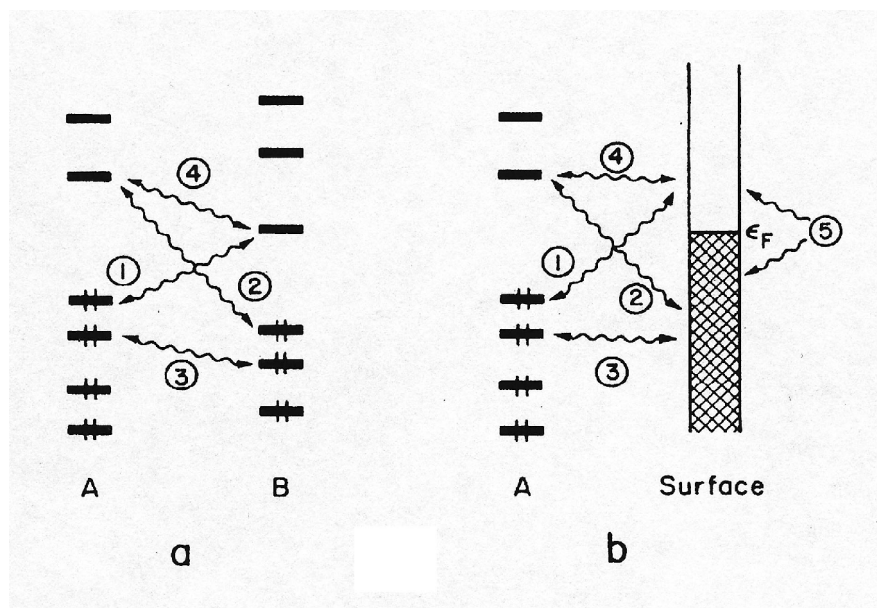
Figure 22: Forces associated with (a) molecule versus (b) surface.
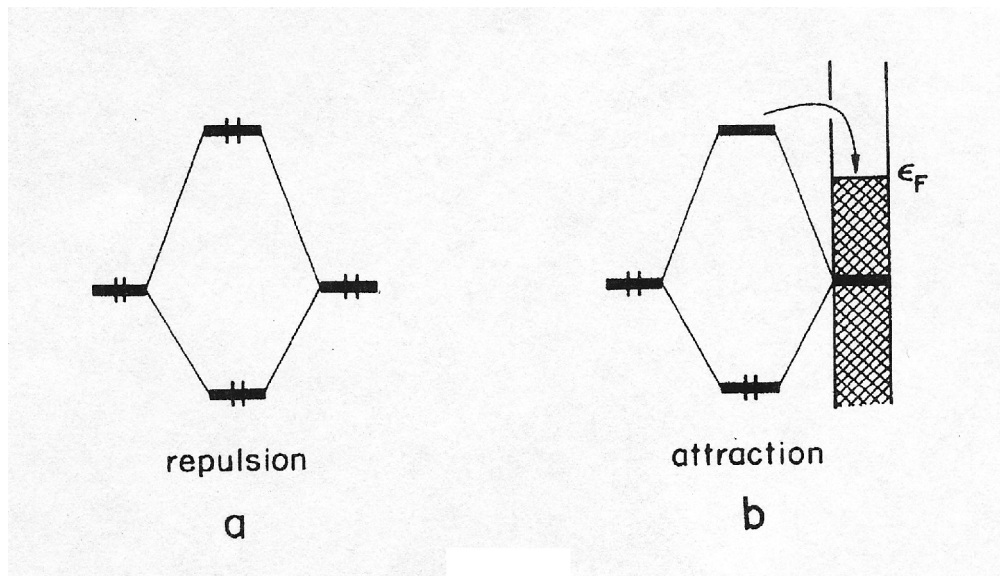
Figure 23: Fermi level influences on a normally repulsive interaction.
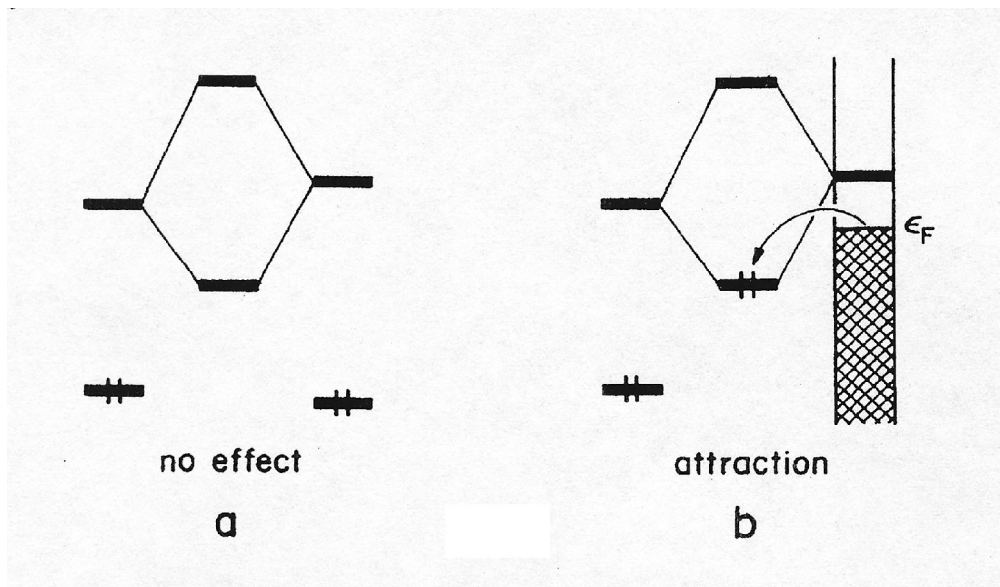
Figure 24: Available states on the adsorbate side accommodate electrons from the Fermi energy.
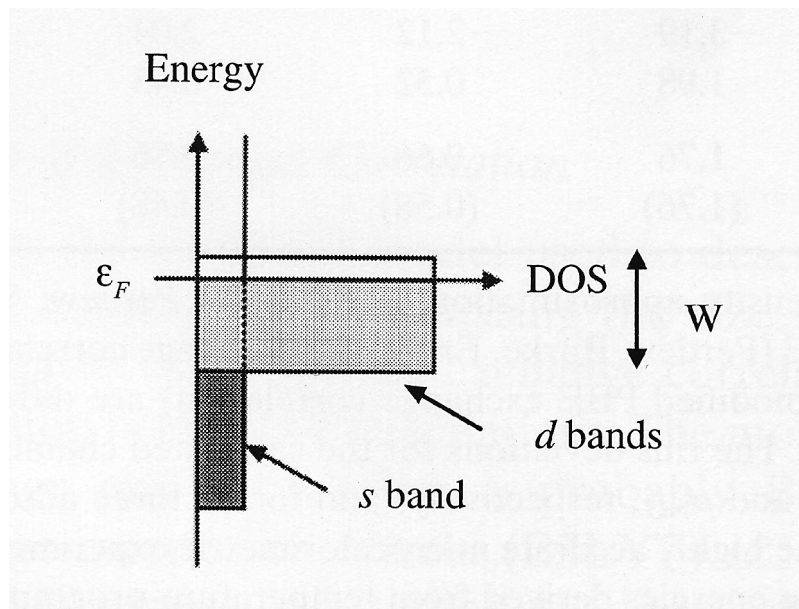
Figure 25: Free electron model expectations for a typical transition metal.
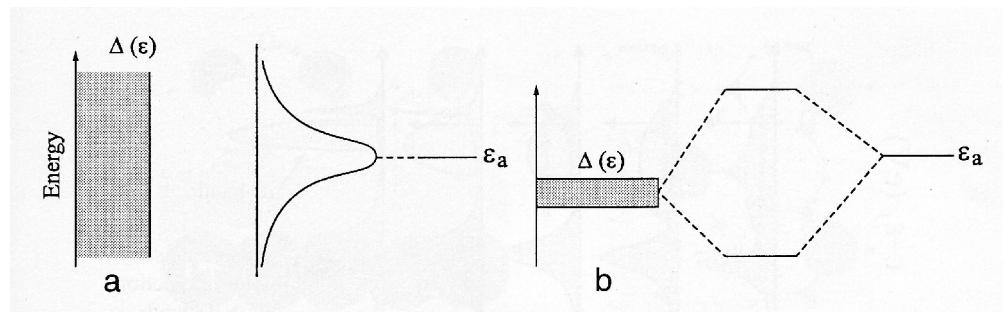
Figure 26: Individual effects of (a) s-band and (b) d-band as adsorption
occurs.
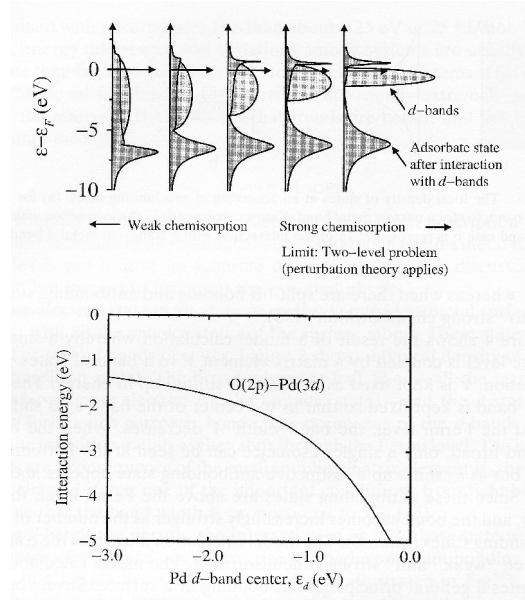
Figure 27: Fundamental d-band definition relative to bond strength for oxygen on a palladium surface.
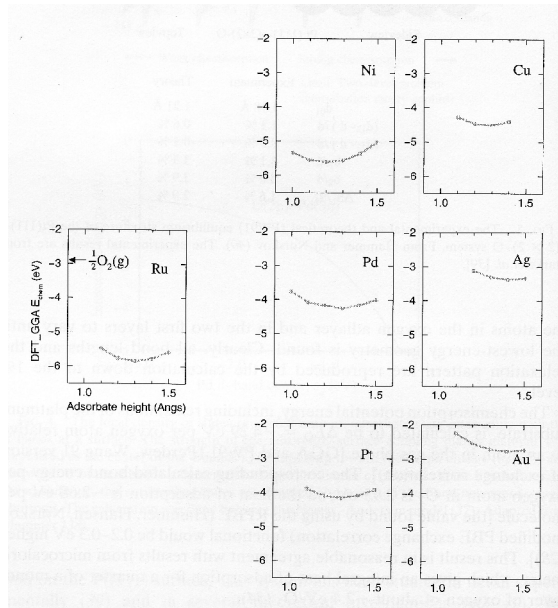
Figure 28: Interaction energies between high valence transition metals and oxygen, arranged in periodic order.
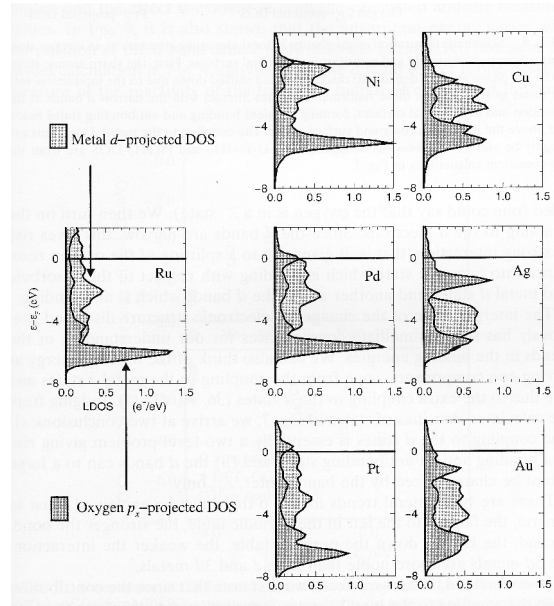
**Figure 29**: Density of states trends exhibited by oxygen on selected transition metal surfaces.
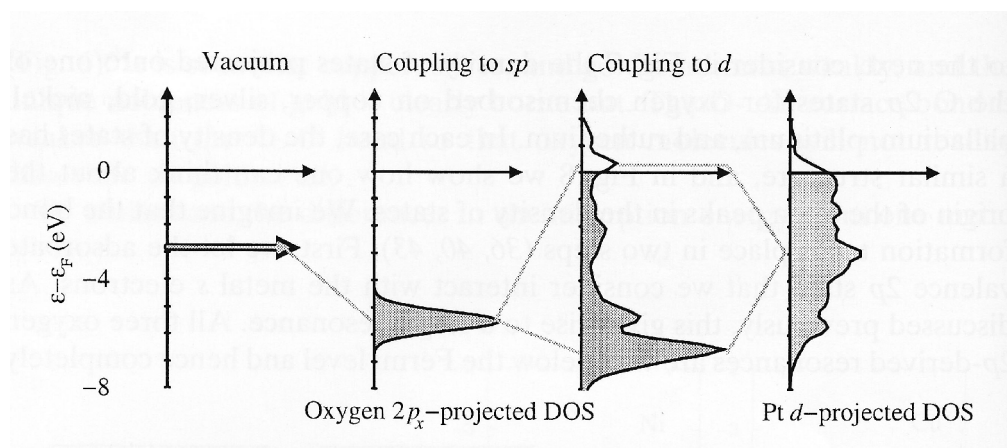
Figure 30: Cummulative forces leading to chemisorption for the oxygen-platinum interaction.
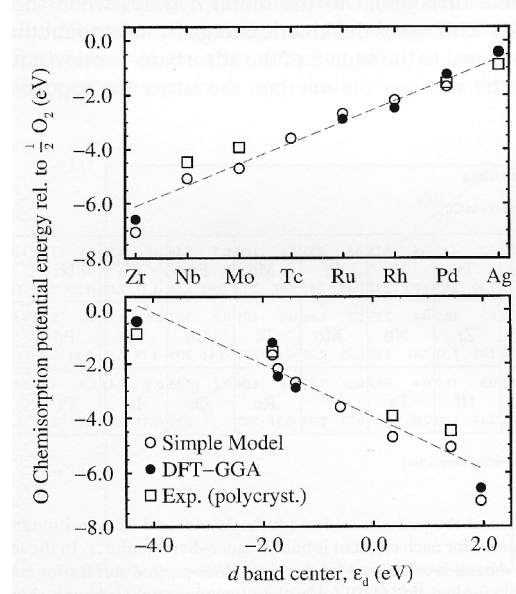
Figure 31: Row type behavior reflected in theoretical and experimental data for oxygen adsorption.
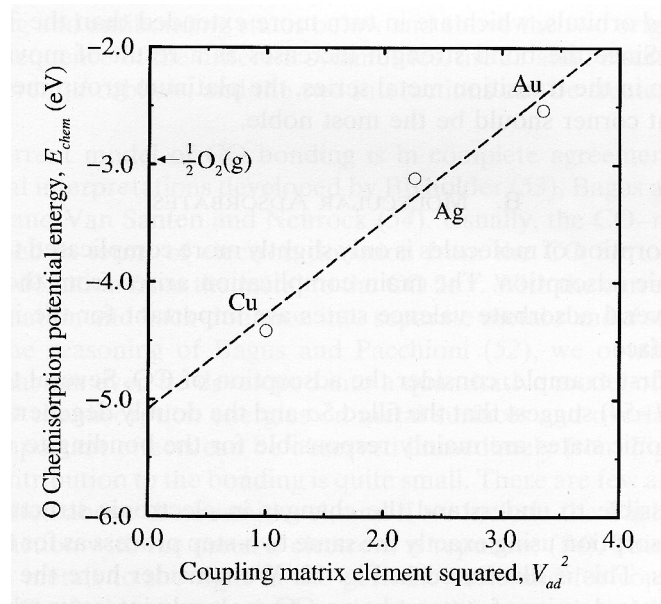

Figure 32: Repulsive charge between noble metals and oxygen attributed to column based periodicity.
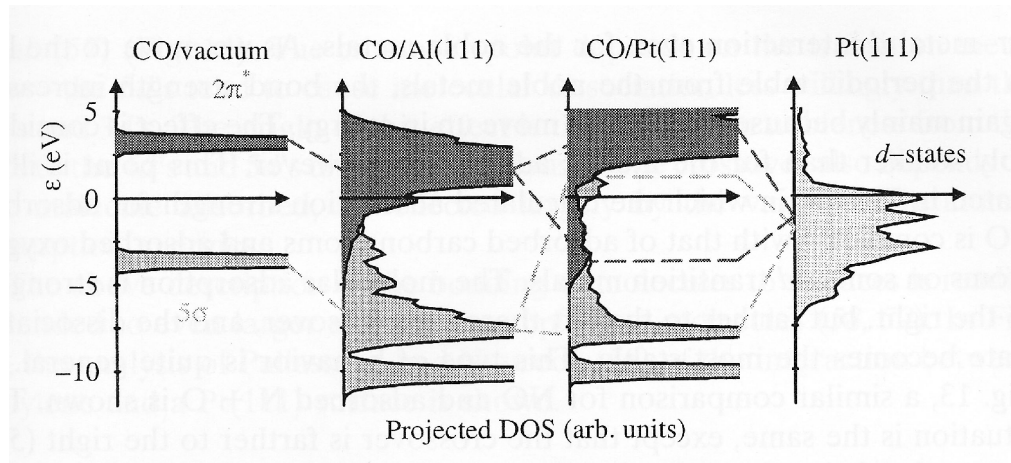
Figure 33: Density of states perception of molecular absorption on main group and transition metal surfaces.
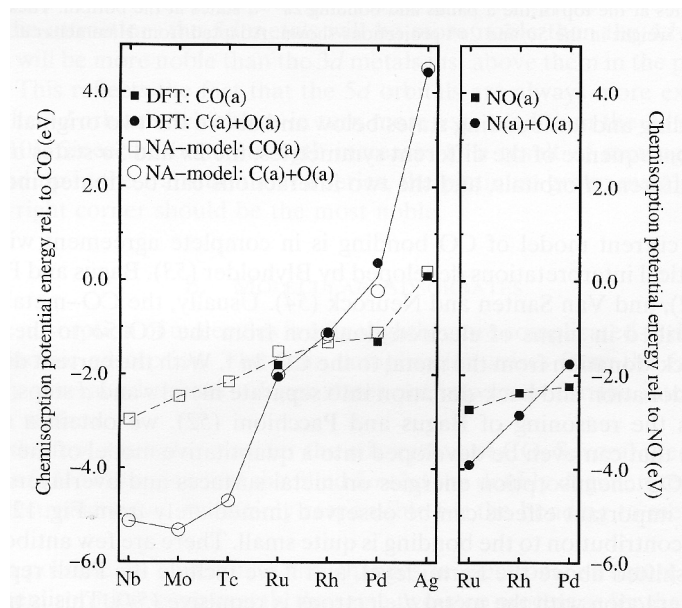
Figure 34: Energy differential between molecular and atomic absorption for second row transition metals.
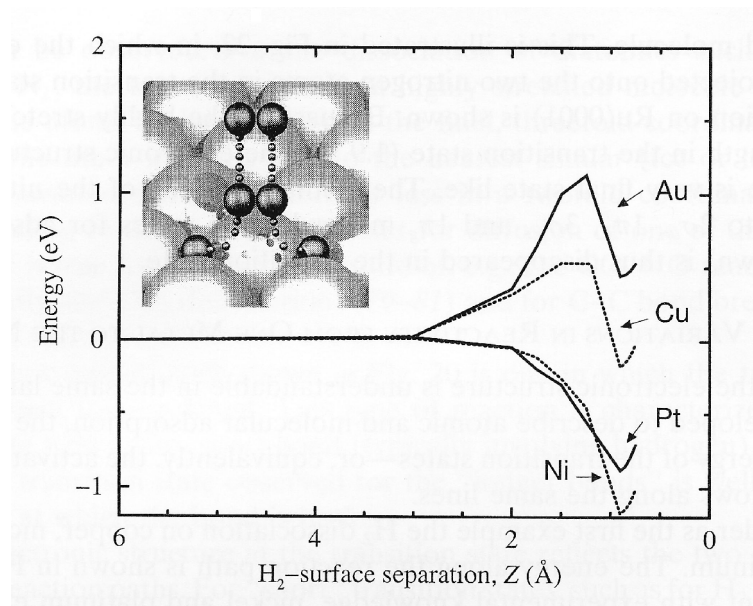
Figure 35: Reaction barrier for hydrogen decomposition on representative transition metal catalysts.
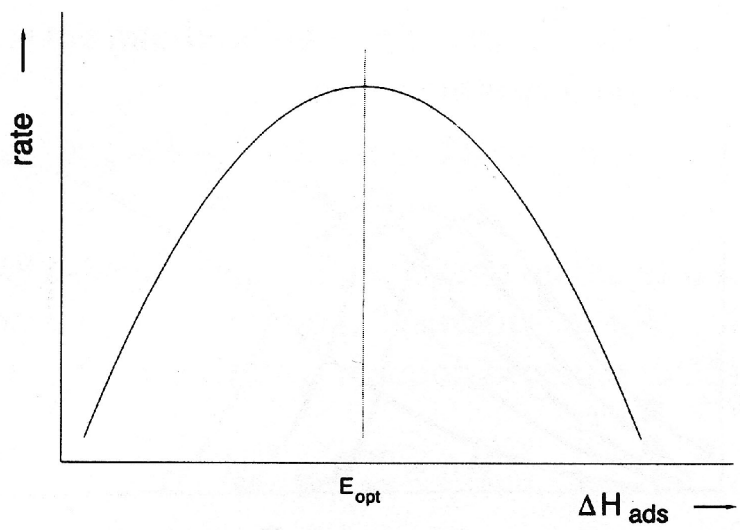
Figure 36: Hypothetical volcano plot used to assess optimal catalytic activity.

References

[1] R. Hoffmann, *Reviews of Modern Physics*, **60**, 601 (1988).

[2] M. T. M. Koper, R. A. Van Santen, and M. Neurock, in *Catalysis and Electrocatalysis at Nanoparticle Surfaces*, A. Wieckowski, E. R. Savinova, and C. G. Vayenas, eds., Marcel Dekker: New York (2003).

[3] B. Hammer and J. K. Nørskov, *Advances in Catalysis*, **45**, 71 (2000).

[4] W. Koch and M. C. Holthausen, *Chemist's Guide to Density Functional Theory*, Wiley: New York (2001).

[5] W. A. Harrison, *Electronic Structure and the Properties of Solids: the Physics of the Chemical Bond*, Freeman: San Francisco (1980).

[6] R. A. van Santen and J. W. Niemantsverdriet, *Chemical Kinetics and Catalysis*, Plenum: New York (1995).